Electronic Supplementary Material

Immunogenic cell death effects induced by doxorubicin improved chemo-immunotherapy via restoration of granzyme B activity

Tao Huang[1,§], Xiaofan Sun[1,§], Yingqiu Qi[1,2,§], Xi Yang[1], Linyao Fan[1], Mengdie Chen[2], Yale Yue[2], Hong Ge[3], Yiye Li[4], Guangjun Nie[4] (✉), Huan Min[1,2] (✉), and Xianfu Sun[1] (✉)

[1] *Department of Breast Disease, The Affiliated Cancer Hospital of Zhengzhou University & Henan Cancer Hospital, Henan Institute of Advanced Technology, Zhengzhou University, Zhengzhou 450008, China*

[2] *Department of Pharmacology, School of Basic Medical Sciences, Zhengzhou University, Zhengzhou 450001, China*

[3] *Department of Radiation Oncology, The Affiliated Cancer Hospital of Zhengzhou University & Henan Cancer Hospital, Zhengzhou 450003, China*

[4] *CAS Key Laboratory for Biomedical Effects of Nanomaterials and Nanosafety & CAS Center for Excellence in Nanoscience, National Center for Nanoscience and Technology, Beijing 100190, China*

[§] *Tao Huang, Xiaofan Sun, and Yingqiu Qi contributed equally to this work.*

Supporting information to https://doi.org/10.1007/s12274-023-5581-6

Address correspondence to Guangjun Nie, niegj@nanoctr.cn; Huan Min, minh@zzu.edu.cn; Xianfu Sun, zlyysunxianfu1256@zzu.edu.cn

1 Materials and methods

Materials: 1,2-Distearoyl-sn-glycero-3-phosphoethanolamine-N-[methoxy(polyethylene glycol)] (DSPE-PEG), and 1,2-distearoyl-sn- glycero-3-phosphoethanolamine-N-[maleimide-(polyethylene glycol)] (DSPE-PEG-MAL) was purchased from Shanghai Ponsure Biotech. Cys-Arg-Gly-Asp (CRGD) peptide (>95%) was purchased from Genscript Biotech co. ltd. Doxorubicin hydrochloride (DOX), cholesterol, indocyanine green (ICG), and lecithin were purchased from Shanghai Macklin Biochemical Technology Co., Ltd. (Shanghai, China). 1,3-benzoxazole-6-carboxylic acid (3034) was purchased from Shanghai Aladdin Biochemical Technology Co., Ltd. PBS, RPMI 1640 medium, and fetal bovine serum (FBS) were purchased from Wuhan Servicebio Technology Co., Ltd. Cell Counting Kit-8 (CCK-8), HRP Conjugated Antibody and BCA kits were purchased from Solarbio Life Science (Beijing, China). Fluorescent dye-conjugated antibodies against mouse CD3 (cat# 100204), mouse CD4 (cat# 100412), mouse CD25 (cat# 102016), mouse CD8 (cat# 100707), mouse CD44 (cat# 103012), mouse CD62L (cat# 104418), mouse CD11c (cat# 117310), mouse CD80 (cat# 104705), mouse CD86 (cat#159203), mouse IFN-γ (cat# 505826), mouse Granzyme B (cat# 515406) were purchase from Biolegend (San Diego, CA, USA). ATP assay kits and Hoechst 33342 were obtained from Beyotime Biotech. Co., Ltd. (Shanghai, China).

Instruments and characterization: Hydrodynamic size distribution and zeta potentials of nanoparticles were measured with a dynamic light scattering (DLS) instrument (Nano-Zs90, Malvern, UK). The Uv-vis absorption spectra of prepared nanomedicines were measured with a UV-vis spectrometer (Ocean Optics, maya2000). The morphology of prepared nanomedicines was imaged with transmission electron microscopy (Hitachi High-Tech, HT7700, Japan). Drug loading and release were analyzed by a high-performance liquid chromatograph (LC5090, Fuli, China). Flow cytometry analysis was performed with a flow cytometer (NovoCyte 2060R, Agilent Technologies, USA). Fluorescence images were obtained by inverted fluorescence microscopy (Nikon ECLIPSE Ti2, Japan) and laser confocal fluorescence microscopy (Carl Zeiss LSM880). In vivo and ex vivo imaging was conducted with an in vivo fluorescent imaging system (IVS Lumina LT series, PerkinElmer, USA).

Cell lines and animals: Luciferase-labeled mouse-derived breast cancer 4T1 (4T1-Luc) cells were incubated in RPMI 1640 medium with 10% fetal bovine serum (FBS) and 1% penicillin/streptomycin. The cells were

cultured in a humidified atmosphere (37 ℃, 5% CO_2). BALB/c mice were purchased from Sibeifu (Beijing) Biotechnology Co., Ltd. All animal experiments were approved by the Care and Use of Laboratory Animals of Zhengzhou University, Zhengzhou, China.

Synthesis of DSPE-PEG-RGD: DSPE-PEG-MAL and peptide CRGD with a molar ratio of 1:2 and catalytic trimethylamine were dissolved in 5 mL of acetonitrile. After stirring at room temperature for 4 h, the solvent of this solution was removed with a rotary evaporator. The obtained sample was further purified by dialysis for 48 h, and freeze-dried for the following experiments and characterization by mass spectrometry.

Preparation of D3RL: The liposome was prepared according to a classical film dispersion method. Briefly, an indicated amount of liposome materials (cholesterol, lecithin, and DSPE-PEG-RGD) and hydrophobic compound 3034 were accurately added into a flask with a 10 mL solution of trichloroethane and methanol with an equal volume. The solution was fully mixed with ultrasound for 10 minutes, and then vacuumed with a rotary evaporator at room temperature. After removing the solvent, a transparent lipid film at the flask bottom was obtained. Subsequently, 4 mL PBS containing a certain amount of DOX was added into the flask with ultrasound and followed by rotating for 2 h at 45 ℃. The obtained mixture was concentrated with a 50 kDa MW cutoff filter (Millipore, USA) unit to remove the free drugs. After resuspending with indicated volume of PBS, the nanomedicine D3RL was obtained, and used for subsequent in vitro and in vivo studies. Other nanomedicines, containing blank liposome, 3034 and DOX-loaded liposome DOX-3034@Lipo (D3L), DOX-loaded liposome DOX@Lipo (DL), 3034-loaded liposome 3034@Lipo (3L) were prepared with DSPE-PEG according to a similar protocol.

Storage stability evaluation: The prepared D3L and D3RL were suspended in PBS with a concentration of 10 mg/mL, and the suspension was stored at 4℃. The hydrodynamic size distribution and zeta potentials of the suspensions were measured every day with the DLS instruments for 7 days.

Release kinetics studies of DOX and 3034: The prepared D3RL was sealed into a dialysis bag (MWCO = 50 KDa, Biotopped), and then transferred into a 50 mL tube containing 20 mL PBS with pH at 7.4 or 6.5. The tube

was then incubated at 37 ℃ and shaken at 100 rpm. At the indicated time intervals, 1 mL of solution was collected and 1 mL of fresh PBS was returned. HPLC was used to detect the concentrations of DOX and 3034 in the solution taken at indicated time points. The release rate (r_n) of 3034 or DOX was calculated according to the following formula:

$$r_n = \frac{20c_n + \sum_{i=1}^{n-1} ci}{m_{initial}} * 100\%$$

Where c_n and c_i are the concentration of 3034 or DOX in the nth and i_{th} collection times. $m_{initial}$ is the amount of initially added 3034 or DOX.

Cytotoxicity evaluation *in vitro*: 4T1-Luc cells were seeded into a 96-well plate at a density of 5× 10^3 cells per well and then incubated for 24 h. Then cells were treated with indicated nanomedicine with an equal concentration of 3034 or DOX for 24 h. Cells were washed twice with PBS and then incubated with fresh 1640 medium with 10% of CCK-8 solution. After incubation for 30 min, the absorbance at 450 nm of each well was measured for the cellular viability calculation.

Cellular uptake *in vitro*. To study the cellular uptake of prepared nanomedicine, 4T1-Luc cells were seeded into a confocal dish at 2 × 10^4 cells per well and incubated overnight. Then cells were treated with DL, D3L, or D3RL with equal DOX for 4 h. Afterwards, the cells were washed with cold PBS three times and fixed with 4% (w/v) cold paraformaldehyde for 15 minutes. Cellular nuclei were stained with Hoechst 33342 for 5 minutes for imaging with a confocal fluorescence microscope. For flow cytometry analysis, 4T1-Luc cells were seeded into a 6-well plate at 2 × 10^5 cells per well and incubated overnight. Then cells were treated with DL, D3L, or D3RL with equal DOX for 4 h Afterwards, the cells were washed with cold PBS three times and collected for flow cytometric analysis.

CRT exposure measurement: To visualize the CRT release, 4T1-Luc cells were seeded in 96-well plates at a density of 3× 10^3 cells per well for 24 h and then incubated with the indicated nanomedicine for an additional 24 h. The cells were fixed with 4% paraformaldehyde for 15 minutes. As for immune staining, cells were sealed with 5% BSA for 20 minutes, stained with CRT antibody for 1 h, and subsequently incubated with FITC-labeled secondary antibody for 40 minutes. Before observing with a fluorescence microscope, cellular

nuclei were stained with Hoechst 33342 for 5 minutes. As for quantitative analysis, flow cytometry was used to determine CRT exposure on the cell membrane surface. In detail, 4T1-Luc cells were seeded in 6-well plates at a density of 2× 10^5 cells per well for 24 h, and then added to the indicated nanomedicine for an additional 24 h. Cells were collected for immunostaining as mentioned above and analyzed by flow cytometry.

HMGB1 release measurement: To measure the release of HMGB1, 4T1-Luc cells were seeded in 96-well plates at a density of 3× 10^3 cells per well for 24 h and then incubated with the indicated nanomedicine for an additional 24 h. Before immune staining, cells were fixed with 4% paraformaldehyde for 15 minutes and sealed with 5% BSA for 20 minutes. As for immunofluorescence staining, cells were incubated with HMGB1 primary antibody for 1 h and then incubated with FITC-labeled secondary antibody for 40 minutes. Before observing with a fluorescence microscope, cellular nuclei were stained with Hoechst 33342 for 5 minutes. As for quantitative analysis, ELISA kits were used to detect the release of HMGB1. Briefly, cells were seeded in 6-well plates at a density of 2× 105 cells per well for 24 h and incubated with the indicated nanomedicine for an additional 24 h. The supernatant of each well was taken, and the released HMGB1 was detected by ELISA kits according to the instructions.

ATP release measurement: To measure the release of ATP, 4T1-Luc cells were seeded in 6-well plates for 24 h at a density of 2× 10^5 cells per well, and then treated with the indicated nanomedicine for an additional 24 h. Cells were washed with PBS and then collected with lysis buffer. The collected cell lysates were centrifuged at 1200 g for 5 minutes and the supernatants were collected, and quantitatively analyzed with an ATP assay kit.

Western blot analysis: 4T1-Luc cells were seeded in 6-well plates at a density of 2 × 10^5 cells per well and incubated for 24 h, followed by being treated with the indicated nanomedicine for an additional 24 h. Afterward, cells were washed with PBS and the total cellular protein was extracted and quantified. Then 30 μg proteins from each group were used for SDS-PAGE electrophoresis and further transferred to the polyvinylidene fluoride (PVDF) membrane. After being blocked, the membrane was incubated with GrB primary antibody overnight, and then incubated with HRP-labeled secondary antibody for 2 h. Finally, the protein blots were imaged and the chemiluminescence signals were detected. GAPDH was chosen as a loading control.

Pharmacokinetics and biodistribution: To study the blood clearance and biodistribution of prepared nano-formulation, a hydrophobic fluorescence dye (indocyanine green, ICG) was used to be loaded in D3L (denoted as ICG-D3L) or D3RL (denoted as ICG-D3RL). Then 4T1-Luc tumor-bearing mice were intravenously injected with free ICG, ICG-D3L, or ICG-D3RL (with an ICG dose of 2.5 mg/kg). Blood was collected at predetermined time intervals, and imaged with an IVIS in vivo imaging system. To study the biodistribution of nanomedicine, 4T1-Luc tumor-bearing mice were intravenously injected with free ICG, ICG-D3L, or ICG-D3RL (with an ICG dose of 2.5 mg/kg), and the mice were imaged at predetermined time intervals with an IVIS in vivo imaging system. After 12 h post-injection, the mice were sacrificed, and tumor tissues with major organs were acquired and imaged by the IVIS in vivo imaging system.

Antitumor effect *in vivo*: 4T1-Luc tumor was implanted into female Balb/c white mice with 6-8 weeks old by subcutaneous injection of 5 × 106 4T1-Luc tumor cells. When 4T1-Luc tumor volume reached approximately 100 mm^3, mice were randomly divided into 6 groups (n=5): (1) PBS, (2) Lipo, (3) DL, (4) 3L, (5) D3L, (6) D3RL. The doses of 3034 and DOX were equally set as 5 mg/kg. Mice were intravenously injected with the indicated nanomedicine for 5 times every two days. To assess the therapeutic efficacy, the body weight of mice and tumor volumes were recorded every other day. During the treatment, the bioluminescence of tumors was acquired at day 0, 5 and 10 using an IVIS system and Living Image Software. Tumor volume was calculated with the formula $V= L\times W^2/2$, where L represents the length and W represents the width of the tumor. At the end of treatment, mice were euthanized, and tumors were collected and fixed with 4% paraformaldehyde and embedded in paraffin for immunofluorescence staining of GrB, Sb9, collagen I, and fibronectin.

Mature DCs in TDLN: Tumor-draining lymph nodes (TDLNs) were collected after treatment for quantification analysis of mature DCs with flow cytometry. Briefly, TDLNs were harvested and immediately smashed, and the obtained cell suspension was passed through a 200-mesh cell strainer and washed with fluorescence-activated cell sorting buffer. Cells were stained with antibodies against CD11c, CD80, and CD86 before flow cytometry analysis.

Quantification of tumor-infiltrating immune cells.: The immune cell populations in tumor tissue after treatment were analyzed by flow cytometry. Briefly, the collected fresh tumor tissues were cut into small pieces

and digested by collagenase IV, hyaluronidase, and DNase at 37 ℃ for 30 min. Then the cells were filtered with a 200-mesh cell strainer to prepare the single-cell suspension. The obtained cell suspension was washed with FACS buffer and stained with antibodies against FITC-CD3, APC-CD4, PE-CD8, PE-Cy7-CD25, PE-Cy7-CD62L or APC-CD44 for flow cytometry analysis. For the analysis of IFN-γ and GrB-producing cells, the obtained cells were incubated with fixation buffer and permeabilization wash buffer followed by staining with FITC-CD3, PE-CD8, PE-Cy7-IFN-γ and APC-GrB antibodies for flow cytometry analysis.

Drug penetration in 4T1-Luc Tumor: The 4T1-Luc tumor was implanted into female Balb/c white mice with 6-8 weeks old by subcutaneous injection of 5×10^6 4T1-Luc tumor cells. When 4T1-Luc tumor volume reached approximately 100 mm^3, mice were randomly divided into 3 groups (n=5): (1) DL, (2) D3L, (3) D3RL. The doses of 3034 and DOX were equally set as 5 mg/kg. Mice were intravenously injected with the indicated nanomedicine for 5 times every two days. 6 h post the last injection, the tumors were collected to prepare frozen tissue sections for subsequent immunofluorescence staining. Cellular nuclei were stained with DAPI, the tumor vessel was stained with FITC-CD31, and the penetrated nanomedicine was self-labeled with the red fluorescence of DOX. The observation of drug penetration was carried out with laser confocal fluorescence microscopy, and semi-quantitatively analyzed with an image J Software.

Histopathology and Hematology examination: Major organs (including heart, liver, spleen, lung, and kidney) and tumor tissues of mice from each group (n = 3) were harvested after treatment, and stained with hematoxylin and eosin (H&E) for a histopathology examination. The blood was collected at the end of treatment, and the plasma was acquired after centrifugation at 4 ℃ for 20 min for blood biochemical analysis. The levels of CK and LDH were determined for heart function evaluation. The levels of ALT and AST were determined for liver function evaluation. The levels of CREA and UREA were determined for kidney function evaluation.

Statistical analysis: All experiments were performed in triplicate unless otherwise indicated. Data were analyzed by GraphPad Prism software. Student's t-test was performed for the statistical analysis of the two groups. Statistical significance values were referred as follows: *, $p<0.05$, **, $p<0.01$, ***, $p<0.001$. ns, no significance.

2 Supporting table and figures

Table S1 Zeta potentials and hydrodynamic sizes of different nanoformulations

Nanoformulations	Zeta (mV)	Size (d.nm)	PDI
Lipo (Lipo)	-26.53±0.91	88.07±6.20	0.19±0.05
DOX@Lipo (DL)	-48.97±0.85	70.18±2.03	0.20±0.03
3034@Lipo (3L)	-43.80±2.17	90.43±2.78	0.19±0.04
DOX-3034@Lipo (D3L)	-42.63±1.26	76.32±6.60	0.18±0.03
DOX-3034@RGD-Lipo (D3RL)	-33.43±0.61	77.71±3.71	0.17±0.02

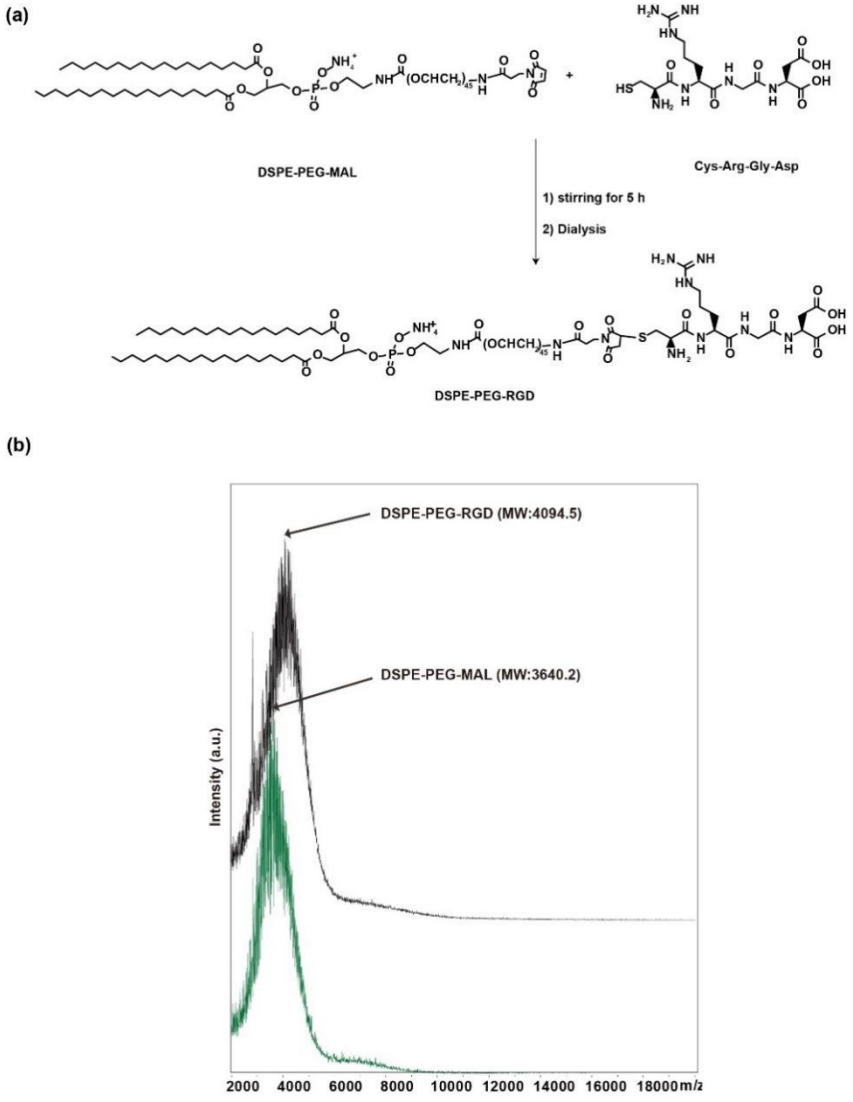

Figure S1 Synthesis and characterization of DSPE-PEG-RGD. (a) Schematic illustration of DSPE-PEG-RGD conjugation by Michael addition reaction between the thiol of cysteine in the Cys-Arg-Gly-Asp peptide and the maleimide at the terminus of the DSPE-PEG-MAL. (b) Mass spectrum analysis of DSPE-PEG-MAL and the prepared DSPE-PEG-RGD. The molecular peak of DSPE-PEG-MAL (3640.2) shifted to 4095.5, indicating the successful preparation of DSPE-PEG-RGD.

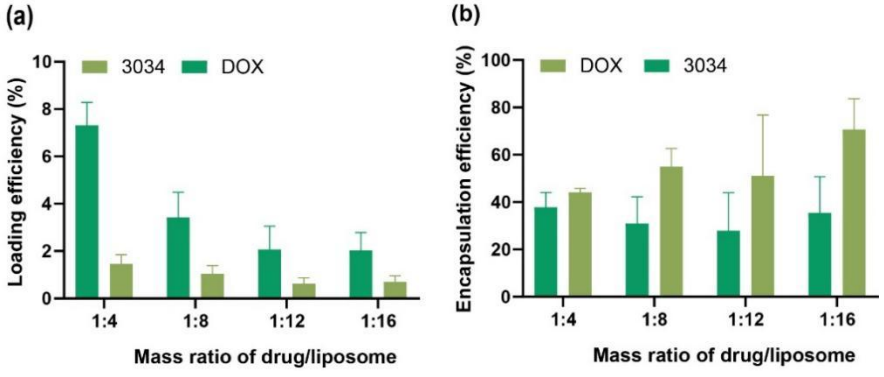

Figure S2 The loading efficiency (a) and encapsulation efficiency (b) of 3034 and DOX in nanomedicines with various mass ratios of drug to the liposome.

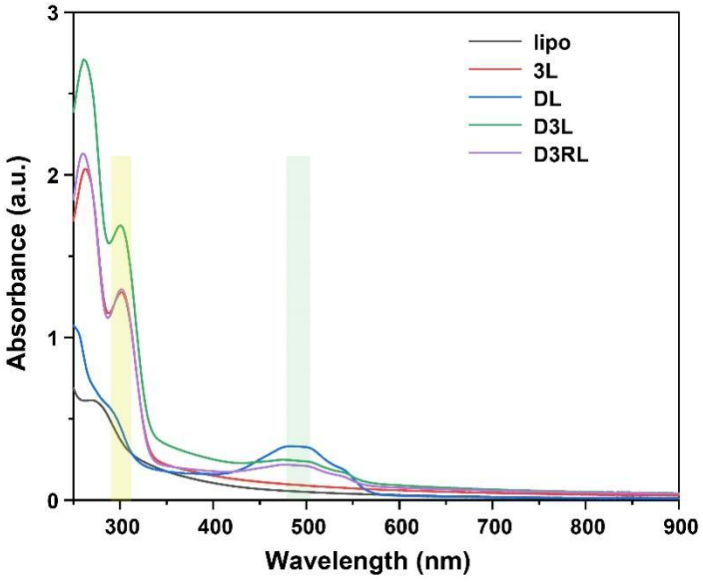

Figure S3. UV-vis absorption spectra of prepared nanomedicines.

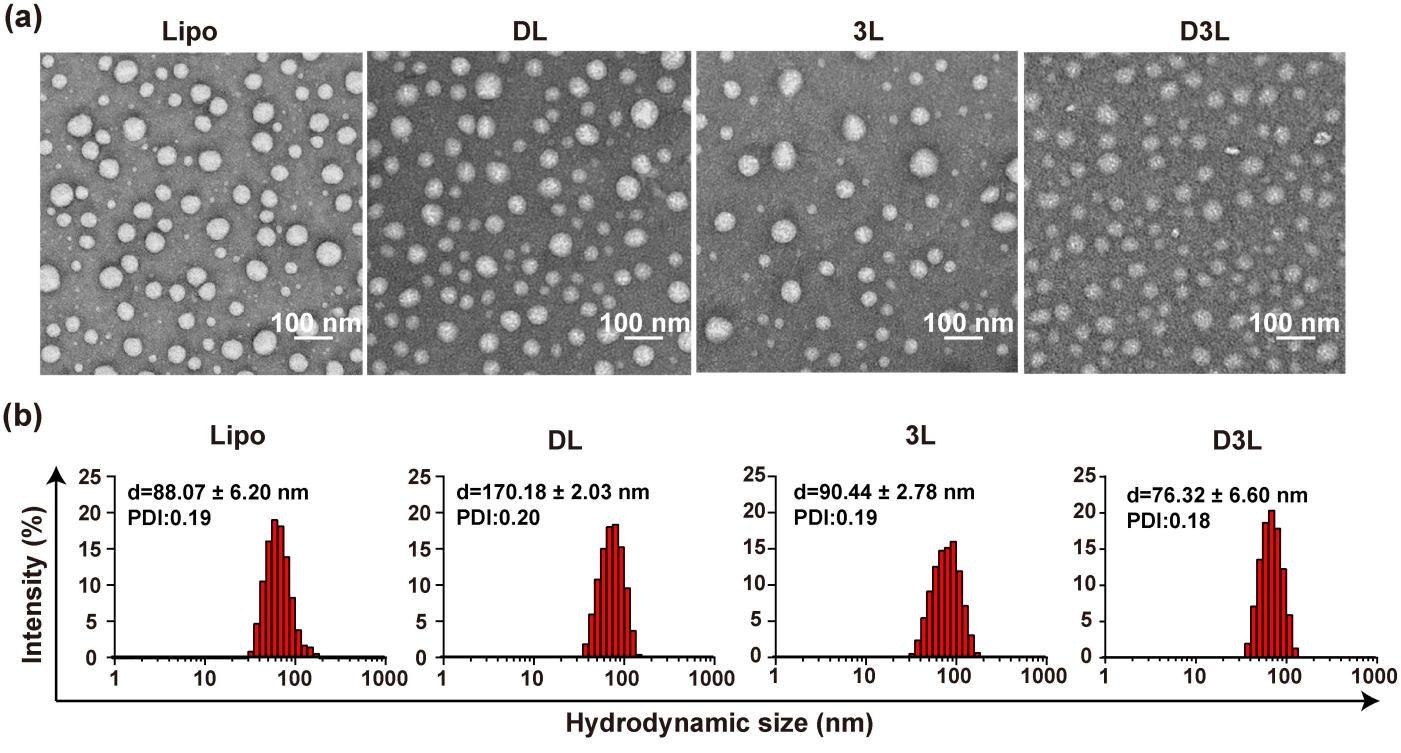

Figure S4 Representative TEM images (a) and hydrodynamic size distribution (b) of Lipo, DL, 3L, and D3L.Scale bar, 100 nm.

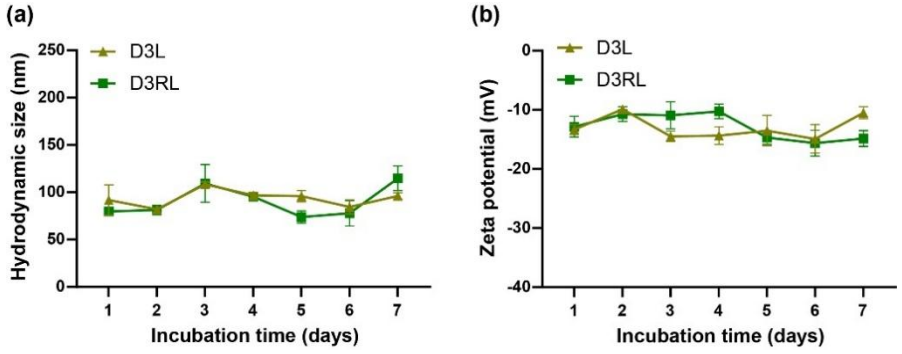

Figure S5 Storage stability evaluation of D3L and D3RL by measuring the hydrodynamic size and zeta potentials during 7 days.

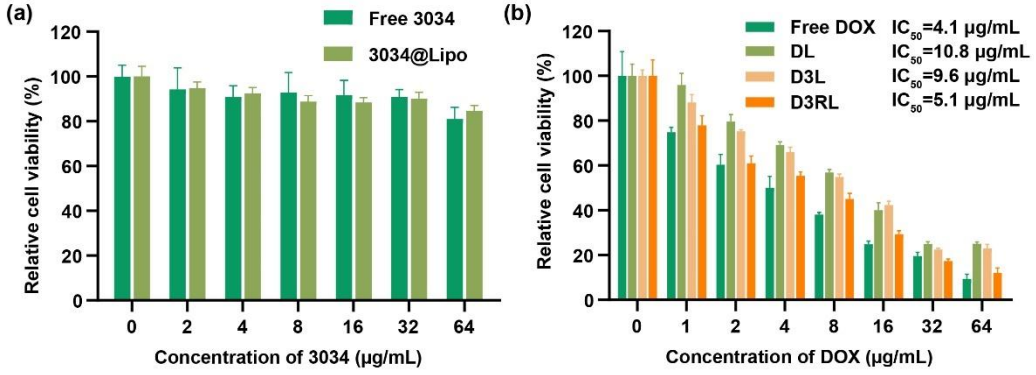

Figure S6 Cytotoxicity evaluation of (a) 3034 containing nanomedicines and (b) DOX containing nanomedicines in 4T1-Luc cells.

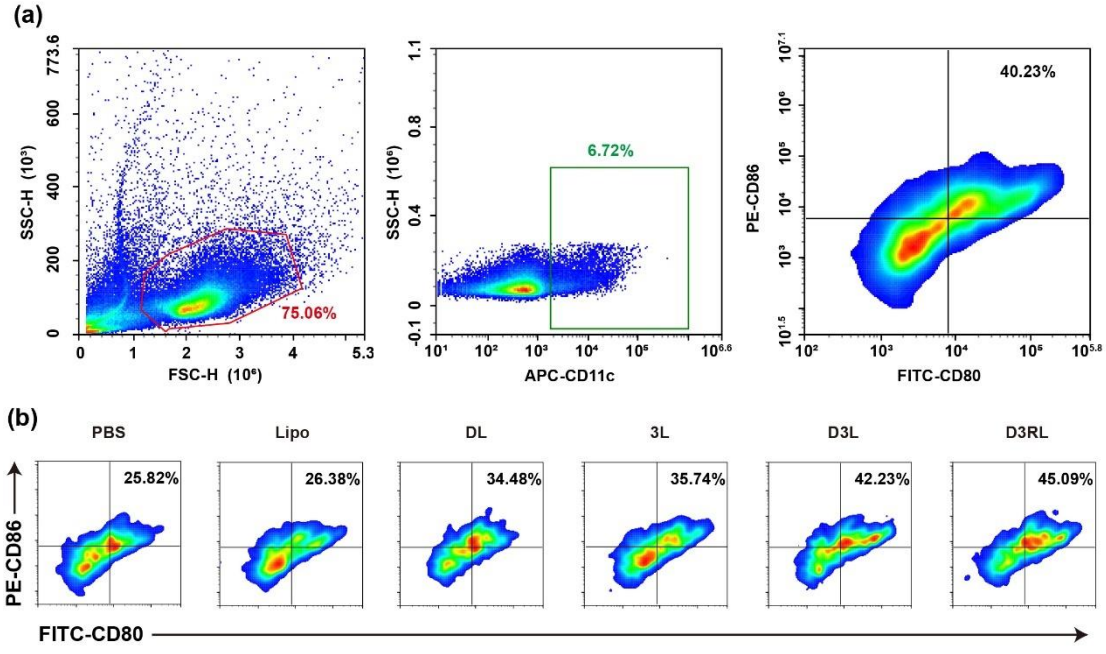

Figure S7 (a) The gating strategy for $CD11c^{+}CD80^{+}CD86^{+}$ cells in tumor-draining lymph nodes (TDLN). (b) Representative flow cytometry analysis of matured DC cells in TDLN from 4T1-Luc tumor-bearing mice with different treatments.

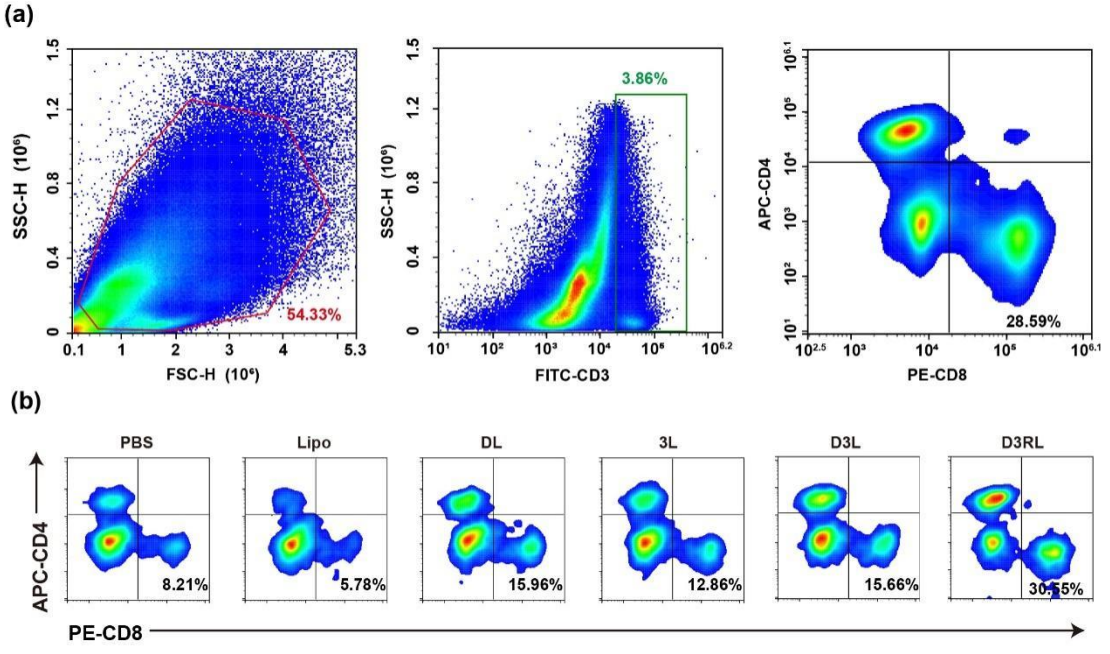

Figure S8 (a) The gating strategy for $CD3^+CD8^+CD4^-$ cells in tumor tissues. (b) Representative flow cytometry analysis of $CD3^+CD8^+CD4^-$ cells in tumor tissues from 4T1-Luc tumor-bearing mice with different treatments.

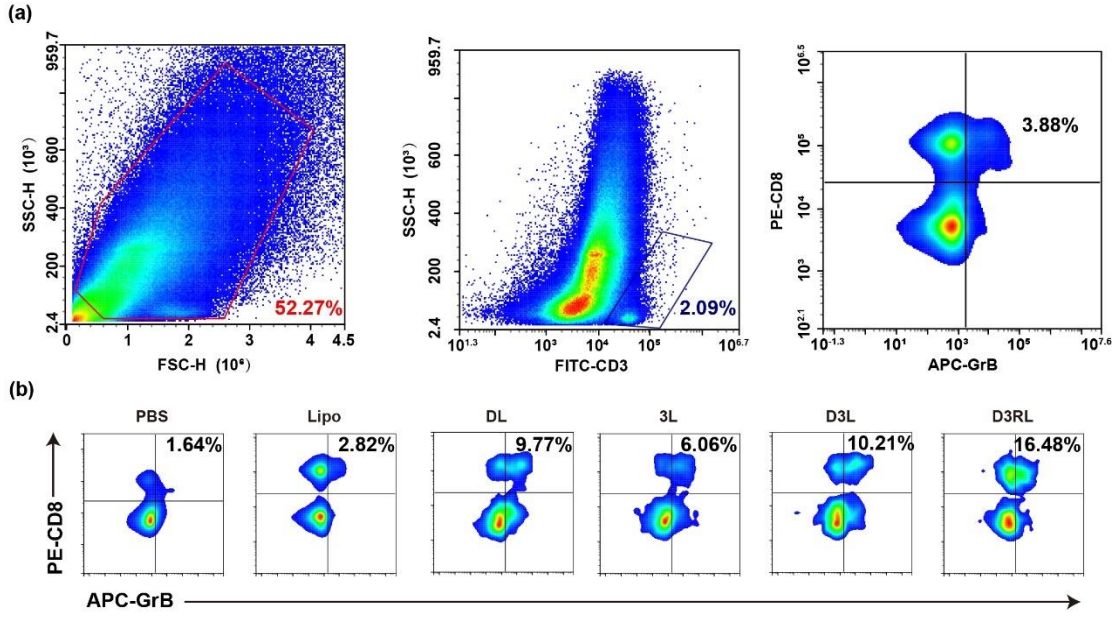

Figure S9 (a) The gating strategy for $CD3^+CD8^+GrB^+$ cells in tumor tissues. (b) Representative flow cytometry analysis of $CD3^+CD8^+GrB^+$ cells in tumor tissues from 4T1-Luc tumor-bearing mice with different treatments.

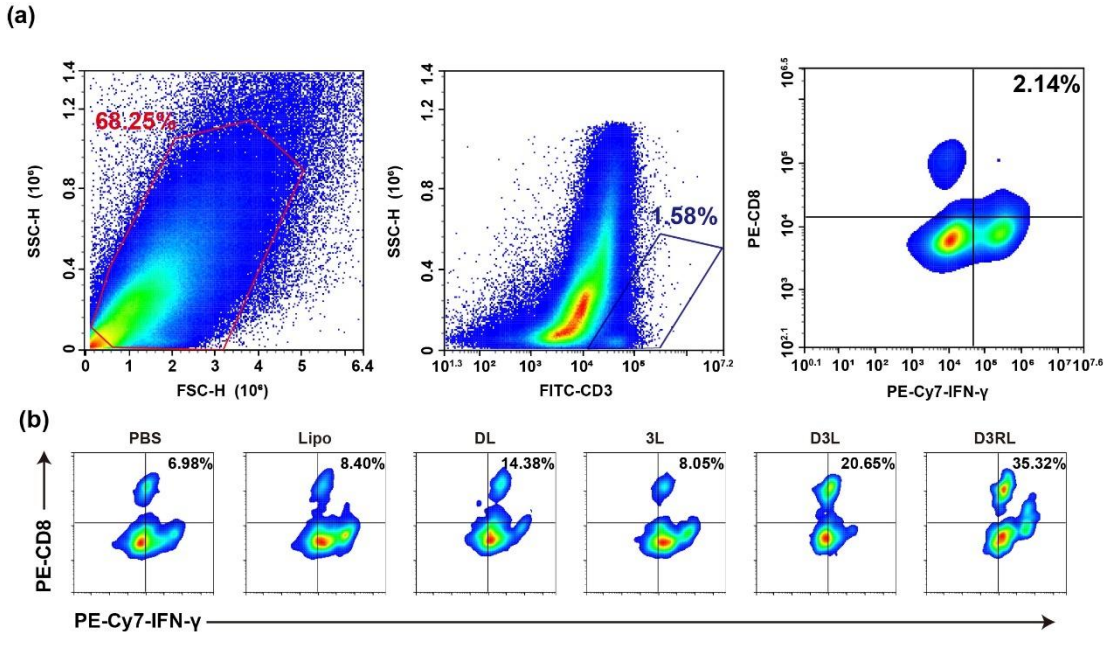

Figure S10 (a) The gating strategy for $CD3^+CD8^+IFN\gamma^+$ cells in tumor tissues. (b) Representative flow cytometry analysis of $CD3^+CD8^+IFN\gamma^+$ cells in tumor tissues from 4T1-Luc tumor-bearing mice with different treatments.

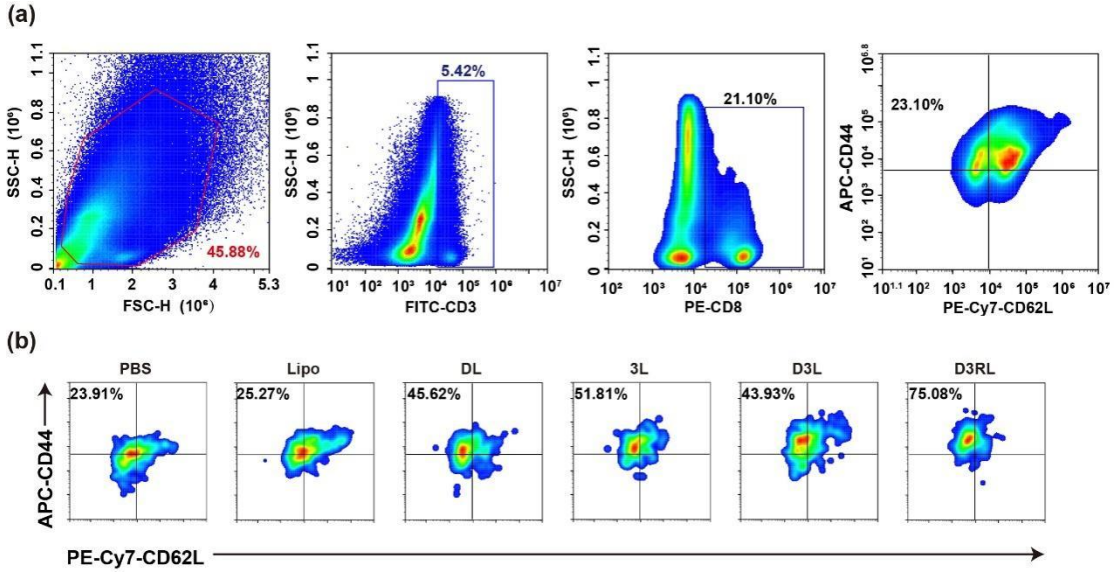

Figure S11 (a) The gating strategy for $CD3^+CD8^+CD62L^-CD44^+$ cells in tumor tissues. (b) Representative flow cytometry analysis of $CD3^+CD8^+CD62L^-CD44^+$ cells in tumor tissues from 4T1-Luc tumor-bearing mice with different treatments.

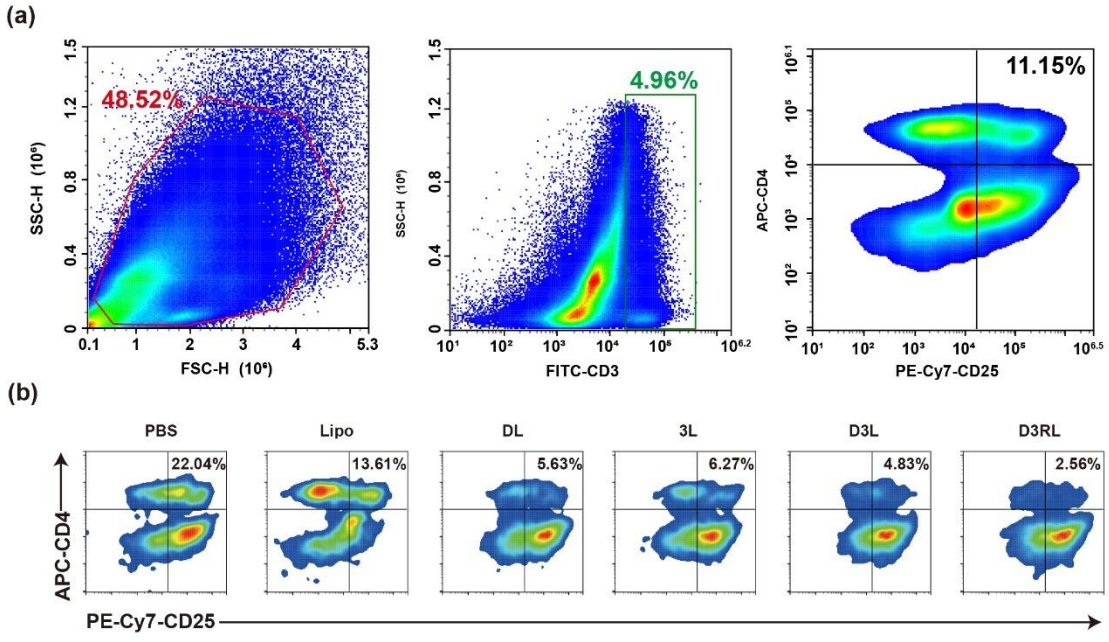

Figure S12 (a) The gating strategy for $CD3^+CD25^+CD4^+$ cells in tumor tissues. (b) Representative flow cytometry analysis of $CD3^+CD25^+CD4^+$ cells in tumor tissues from 4T1-Luc tumor-bearing mice with different treatments.

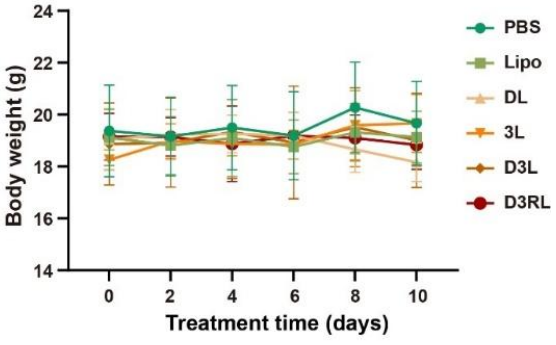

Figure S13 Body weight profiles of 4T1-Luc tumor-bearing mice with different treatments during the trials.

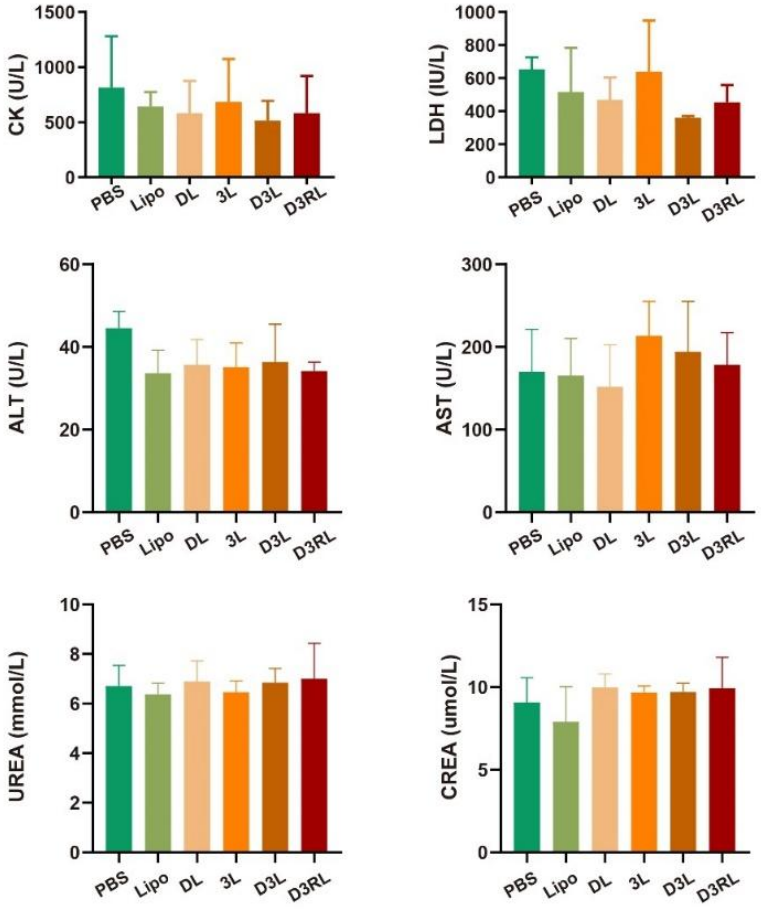

Figure S14 Serum biochemistry analysis of 4T1-Luc tumor-bearing mice with different treatments to evaluate the cardiac, liver, and kidney functions (n = 3). CK (creatine kinase) and LDH (lactic dehydrogenase) are indicators of cardiac function; ALT (alanine aminotransferase) and AST (aspartate aminotransferase) are indicators of hepatic function; BUN (blood urea nitrogen) and CREA (creatinine) are indicators for kidney function.

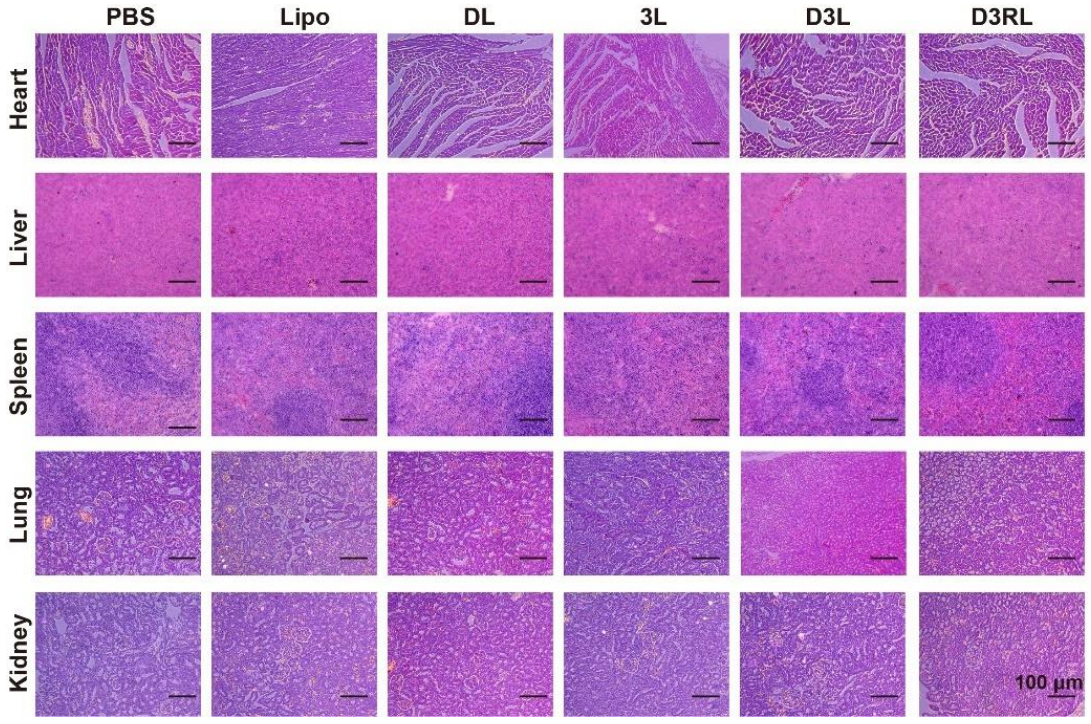

Figure S15 Representative H&E staining images of major organs (including heart, liver, spleen, lung, and kidney) from 4T1-Luc tumor-bearing mice with different treatments. Scale bar, 100 μm.